Hindawi Publishing Corporation
International Journal of Photoenergy
Volume 2008, Article ID 258631, 8 pages
doi:10.1155/2008/258631

Research Article

The Effect of Sulphate Doping on Nanosized TiO_2 and MoO_x/TiO_2 Catalysts in Cyclohexane Photooxidative Dehydrogenation

P. Ciambelli, D. Sannino, V. Palma, and V. Vaiano

Dipartimento di Ingegneria Chimica e Alimentare, Università di Salerno, 84084 Fisciano (SA), Italy

Correspondence should be addressed to P. Ciambelli, pciambelli@unisa.it

Received 30 August 2007; Accepted 29 December 2007

Recommended by Leonardo Palmisano

The effect of sulphate doping of titania in promoting activity and selectivity of MoO_x/TiO_2 catalysts for the cyclohexane photooxidative dehydrogenation has been investigated in a gas-solid fluidized bed reactor. Sulphate and/or molybdate-modified titania catalysts were prepared by incipient wet impregnation of nanosized (5–10 nm crystallite size) samples. At 60% of titania surface coverage by MoO_x, sulphate surface density was obtained up to 19 μmol/m^2 without formation of MoO_3. The catalysts were characterized by N_2 adsorption-desorption at -196°C, micro-Raman and UV-visible reflectance spectroscopy, thermogravimetric analysis coupled with mass spectroscopy (TG-MS), and mass titration. Unsulphated and sulphated titania are both active in cyclohexane total oxidation, but sulphate doping of titania has a detrimental effect on the reaction rate. On Mo-based catalysts, polymolybdate species enabled sulphated titania to convert cyclohexane to benzene (99% selectivity) and cyclohexene, reducing at zero the formation of CO_2. Cyclohexane conversion to benzene is almost linearly dependent on sulphate surface density, resulting in enhanced yield to benzene. The enhanced photooxidative dehydrogenation activity and benzene yield by sulphate doping could be attributed to the increase of surface acidity and, as a consequence, of cyclohexane adsorption.

1. INTRODUCTION

Recently, growing interest has been addressed to novel processes for the synthesis of chemicals by reversing the final goal of the photocatalytic oxidation process—enhancing the selectivity to partially oxidized products so much that the process could be used for their production. Therefore, since one of the main goals of the 21st century chemistry is to replace environmentally hazardous processes, selective photocatalytic partial oxidation can play a key role in this evolution, offering an alternative green route for the production of organics.

Titanium dioxide is the semiconductor most used in photocatalysis because of its high photocatalytic activity allowing to realize the abatement of pollutants both in liquid and gas phases [1–4]. It has been reported that the introduction of foreign species into TiO_2 leads to a dramatic change in activity of the photocatalytic process. In particular, SO_4^{2-}/TiO_2 shows higher photocatalytic activity than unsulphated titania for a large variety of organic compounds [5]. Fu et al. [6] showed that the improved photoactivity of sulphated titanium dioxide was due to a greater surface area as well as a larger fraction of anatase phase which is more active than rutile for the photocatalytic application. In the presence of metal oxides such as WO_3, the surface acidity of TiO_2 was increased, resulting in enhanced photocatalytic activity [7]. The formation of acid sites increases the adsorption strength of different organics, that it is believed to contribute to enhance the photocatalytic activity.

The most of studies on photocatalytic reactions for organic synthesis deals with slurry systems. In contrast, selective oxidation in gas phase with molecular oxygen is still a real challenge to current research. Few examples of selective photocatalytic oxidative conversion of organic substrates in gas phase on modified titania-based catalysts have been reported such as alkane and cycloalkane oxidation [8–10], and olephin epoxidation [11, 12]. However, a significant enhancement of catalytic activity and energy efficiency is necessary for such application of photocatalysis. Recently, we have shown that benzene is obtained with high selectivity by

Table 1: List of catalysts and their characteristics.

Catalyst	MoO_3 wt%	SO_3^* wt%	Surface area m^2/g	MoO_3 density $\mu mol/m^2$	SO_4 density $\mu mol/m^2$
PC500	—	0.55	345	—	0.17
PC500S10	—	11	241	—	4.8
PC500S18	—	19	169	—	11.7
24MoPC500	23.8	0.3	202	8.1	0.15
17MoPC500S10	16.6	10	144	8.0	7.3
12MoPC500S18	11.7	18	99	8.1	18.9

* Evaluated by TG-MS analysis.

photooxidative dehydrogenation of cyclohexane on MoO_x/TiO_2 catalysts in a gas-solid fixed [10] or, better, fluidized bed reactor [13, 14]. The active phases are octahedral polymolybdate species on titania surface [10]. Moreover, we found that the presence of sulphate species on the surface of different titanias (2.4 wt% maximum SO_4 content) enhances the benzene yield as more as higher is the sulphate content evidencing a synergic effect of sulphate and molybdate species [15]. It was also shown that the presence of sulphate increases surface acidity as the sulphate surface density increases. The addition of sulphate to MoO_x/γ-Al_2O_3 catalysts was found to promote the selective mono-oxidative dehydrogenation of cyclohexane to cyclohexene, demonstrating the possibility of finely tuning the process selectivity [16]. Maximum cyclohexane conversion and cyclohexene yield of 11% were obtained for SO_4 content of 2.4 wt% at 120°C. Physicochemical characterization of catalysts indicated the presence of both octahedral polymolybdate and sulphate species on alumina surface as previously found for titania. Increasing sulphate load, thermogravimetry evidenced the presence of up to three sulphate species of different thermal stability. We concluded that the lower activity observed at high sulphate content is likely due to polymolybdate decoration by sulphates [16].

In this paper, we focus the attention on the effect of sulphate doping of nanosized TiO_2 on the photocatalytic oxidative dehydrogenation of cyclohexane to cyclohexene and benzene on MoO_x/TiO_2 in a gas-solid fluidized bed reactor.

2. EXPERIMENTAL

Anatase titania with crystallites size ranging from 5 to 10 nm (PC 500 provided by Millenium Inorganic Chemicals, Stallingborough, United Kingdom) was used as catalyst support. The preparation procedure for catalyst samples (MoPCs) containing various amounts of molybdenum oxide and sulphate consisted of two steps. The first step was the impregnation of the support with an aqueous solution of ammonium sulphate. The suspension was dried under stirring at 80°C to complete removal of excess water. The sample turned into sulphate doped titania by calcination at 300°C for 3 hours. The second step was the impregnation of the sulphated sample with an aqueous solution of ammonium heptamolybdate $(NH_4)_6Mo_7O_{24}\cdot 4H_2O$, drying at 120°C for 12 hours and calcination in air at 400°C for 3 hours.

Photocatalysts characterization was performed by different techniques. Thermogravimetric analysis (TG-MS) of powder samples was carried out in air flow with a thermoanalyzer (Q600, TA) in the range 20–1100°C at 10°C/min heating rate. Specific surface area was evaluated by N_2 adsorption-desorption isotherms at −196°C with a Costech Sorptometer 1040. Powder samples were treated at 180°C for 2 hours in He flow (99.9990%) before testing. Laser Raman spectra of powder samples were obtained with a dispersive micro-Raman (Invia, Renishaw), equipped with 785 nm diode laser, in the range 100–2500 cm^{-1} Raman shift. UV-Vis reflectance spectra were obtained with a Perkin Elmer Spectrometer Lambda 35 using an RSA-PE-20 reflectance spectroscopy accessory (Labsphere Inc., North Sutton, NH, USA). All spectra were performed using an 8° sample positioning holder, giving total reflectance relative to a calibrated standard SRS-010-99 (Labsphere Inc.). The reflectance data were reported as $F(R_\infty)$ values from Kubelka-Munk theory versus the wavelength [17]. Equivalent band gap determinations were made by plotting $[F(R_\infty) * h\nu]^2$ versus $h\nu$ (eV) and calculating the x intercept of a line passing through $0.5 < F(R_\infty) < 0.8$. The zero point charge (ZPC) of supports and catalysts was determined by mass titration according to Noh and Schwarz [18].

Photocatalytic tests were carried out feeding a fluidized bed photoreactor [19] with 830 (stp) cm^3/min N_2 stream containing 1000 ppm cyclohexane, 1500 ppm oxygen, and 1600 ppm water. The composition of the inlet and outlet gases was measured by an online quadrupole mass detector (TraceMS, ThermoFinnigan) and a continuous CO-CO_2 NDIR analyser (Uras 10, Hartmann & Braun). The reactor was illuminated by four UV light sources (eye mercury lamp, 125 W) in a dark box. The temperature was set at 120°C after a screening in the range 40–160°C [19]. In order to achieve fluidization conditions, 14 g of catalyst mixed with 63 g of α-Al_2O_3 (Aldrich, Milano, Italy 10 m^2/g, 50 μm Sauter diameter) were loaded to the reactor. UV sources were activated after the complete adsorption of cyclohexane on catalyst surface in dark conditions.

3. RESULTS AND DISCUSSION

3.1. Catalyst characterization

The nominal MoO_3 and sulphate content together with the specific surface area (S.S.A) of the photocatalysts are reported in Table 1.

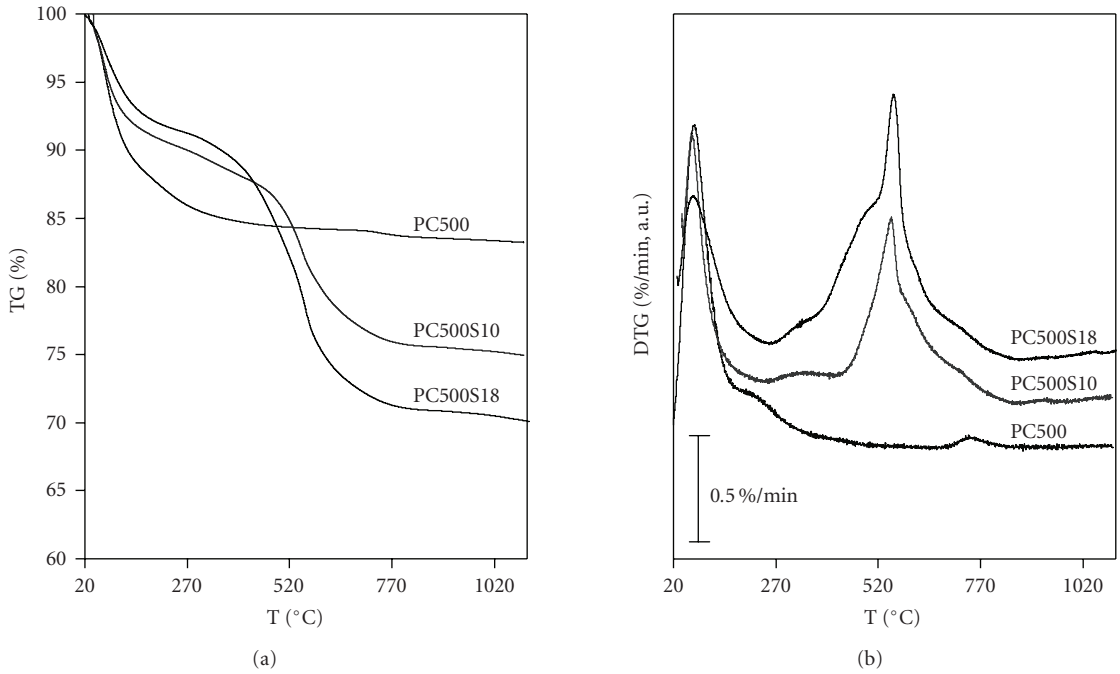

Figure 1: TG (a) and DTG (b) curves of PC500, PC500S10, and PC500S18 catalysts.

Both SO_4 and MoO_3 surface densities were evaluated with respect to the surface area values of the calcined catalysts. All MoPCs were designed to reach about 60% monolayer coverage of titania surface (about 8 μmol/m^2).

Thermogravimetric curves of PC500, PC500S10, and PC500S18 are reported in Figure 1.

Three main steps of weight loss are recognized: (i) the first one associated with hydration water desorption, (ii) the second one related to the removal of OH^- surface groups of titania, (iii) the last one attributed to the decomposition of sulphate species giving rise to gaseous SO_3 as identified from its characteristic fragments m/z = 48 and 64 (not reported). The latter step ranges from 690°C to 840°C for PC500, while downshifts to 420–855°C and 375–850°C for PC500S10 and PC500S18, respectively. By analyzing the first derivative curves in the region of sulphate loss, only one peak centered at 741°C is observed on PC500, while PC500S10 and PC500S18 show three peaks at 552, 599, 717°C and at 477, 555, 730°C, respectively. It has been reported [20] that sulphated TiO_2 shows different regions of sulphate loss, the lowest temperature peak being attributed to a more weakly bonded sulphate species, the highest temperature peak to a more strongly bonded sulphate. The structure of metal oxide bonded sulphate is still subject of investigation in the literature. Jin et al. [20] proposed that sulphate would be coordinated to the titania surface as bidentate anion, Bensitel et al. [21] and Waqif et al. [22] described a structure in which sulphate, at lower content, would be bonded to the metal through three oxygen atoms. Moreover, the sulphate coordination to the surface depends on the dehydration state of the surface and then on the temperature. Increasing temperature and sulphate content, polynuclear sulphates (polysulphates, $S_2O_7^-$, etc.) can be formed.

TG and DTG curves of 24MoPC500, 17MoPC500S10, and 12MoPC500S18 are displayed in Figure 2. All the samples show a decomposition step starting from about 700°C; the onset of weight loss shifts slightly at higher temperature increasing the sulphate load. The estimated amount of weight losses of the three samples well agrees to the nominal MoO_3 content reported in Table 1, allowing the attribution of this step to Mo oxide sublimation, reported to occur in the range 800–1000°C on MoO_x/Al_2O_3 catalysts [23].

The DTG curve of 24MoPC500 shows a single high temperature peak, centered at 624°C due to sulphate decomposition. We attribute the decreasing of decomposition temperature with respect to PC500 to the presence of MoO_x species, similarly as we previously found for WO_x/TiO_2 catalysts [24]. For 17MoPC500S10, in addition to a DTG peak at about 584°C two overlapping peaks appear, with maximum at 466°C and 525°C, likely due to different surface sulphates. Similar DTG peaks, centered at 455°C, 573°C, and 630°C, are shown by 12MoPC500S18.

UV-Vis DRS spectra of all the photocatalysts are reported in Figure 3. When supported on sulphated titania, Mo species absorption bands are difficult to distinguish, as previously reported [16]. However, the presence of MoO_3 crystallites (main band at 360 nm) on the catalysts was not detected. Sulphate doping increases the overall UV absorption of all the samples (Figure 3), correspondent to a slight increase in equivalent band gap energies, reported for MoPCs in Table 2. At similar sulphate level, the partial surface coverage with MoO_x leads to a small decrease in the equivalent band gap energies with respect to the relevant support.

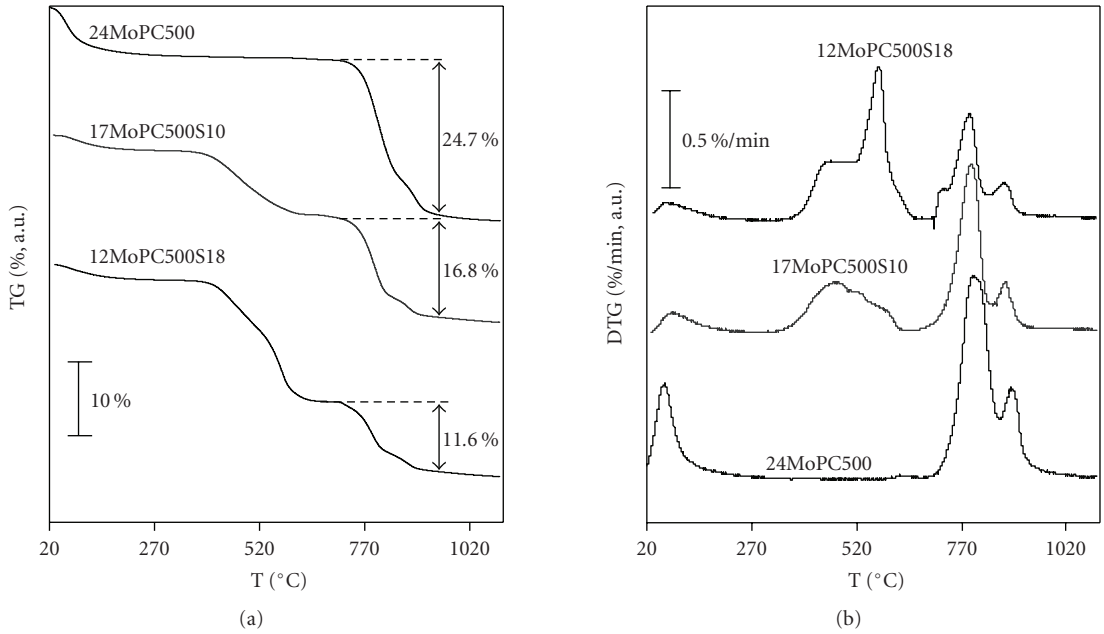

Figure 2: TG (a) and DTG (b) curves of 24Mo PC500, 17MoPC500S10, and 12MoPC500S18 catalysts.

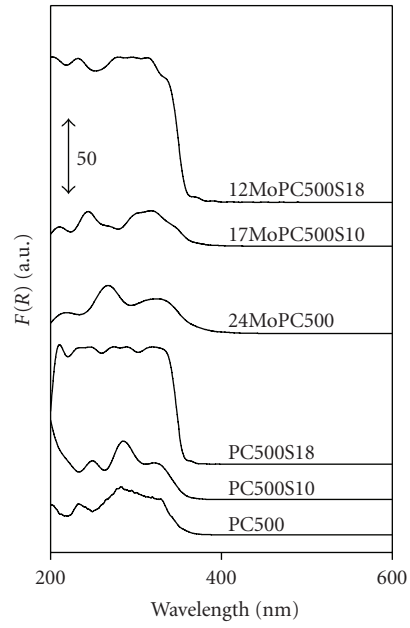

Figure 3: UV-Vis DRS spectra of PC500, PC500S10, PC500S18, 24MoPC500, 17MoPC500S10, and 12MoPC500S18 catalysts.

Increasing the sulphate content of titania, the values of ZPC (Table 2) decrease from 5.8 for PC500 to 2.2 for PC500S18. Also the presence of molybdenum confers, in all cases, stronger acidity, indicated by the ZPC values of MoPCs catalysts, as reported in [15].

The Raman spectra of PC and MoPC samples are reported in Figures 4(a) and 4(b), respectively. PC500S10 and PC500S18 exhibit a band around 986 cm^{-1} assigned to symmetric stretching mode ν_1 of sulphate belonging to point group Td [25]. The signal at about 1012 cm^{-1} for PC500S10 and at 1018 cm^{-1} for PC500S18 is due to the S=O bonds of isolated sulphates [26].

Broad bands around 1050 and 1180 cm^{-1} are due to removal of degeneration of $\nu 3$ mode, owing the symmetry lowering with the coordination to the titania surface hydroxyl groups as bidentate anion. The upshift of S=O Raman band could indicate the strengthening of double bond due to the formation of polynuclear sulphates [25]. On MoPCs, the absence of bulk molybdena bands at 819 and 995 cm^{-1} [27] for all Mo-based catalysts confirms the absence of MoO_3 crystallites. Moreover, a complex band with several contributions in the range 940–1030 cm^{-1} is observed. For 24MoPC500 the maximum is at 984 cm^{-1}, with shoulders at 960 and 967 cm^{-1}. For 17MoPC500S10 the complex band is sharpened, with an additional strong signal at 992 cm^{-1}, overimposed to 970, 980, and 984 cm^{-1} shoulders. For 12MoPC500S18, 978 and 982 cm^{-1} signals with a maximum at 996 cm^{-1} are present, characteristic of polymolybdenyl species [28]. The Mo=O asymmetric stretching modes of hydrated octahedrally polymeric species lay in the range 940–988 cm^{-1} [29] with nuclearity ranging between 7 and 12. Wachs [28] reported that in hydrated conditions $Mo_8O_{26}^{4-}$ presents a Raman Mo=O band at 963 cm^{-1} on titania. The presence of polymeric octahedral species and sulphate can be thus recognised. 984 and 996 cm^{-1} signals could be ascribed to the surface sulphates, considering the absence of 820 cm^{-1} band of MoO_3 crystallites. Bands at 993, 1009, and 1111 cm^{-1} have been assigned to the S–O stretching vibrations of SO_4^{2-} species on CeO_2 [30]. The structure of sulphate species responsible for the band at 993 cm^{-1} cannot be definitely determined and thus requires further investigations.

Table 2: Equivalent band gap energy, ZPC values, and amount of adsorbed cyclohexane in dark conditions for all catalysts.

Catalyst	Equivalent band gap energy eV	ZPC pH unit	Adsorbed cyclohexane μmol/m^2
PC500	3.3	5.8	0.048
PC500S10	3.3	4.1	0.034
PC500S18	3.4	2.2	0.026
24MoPC500	3.0	3.4	0.09
17MoPC500S10	3.2	2.2	0.14
12MoPC500S18	3.3	1.2	0.22

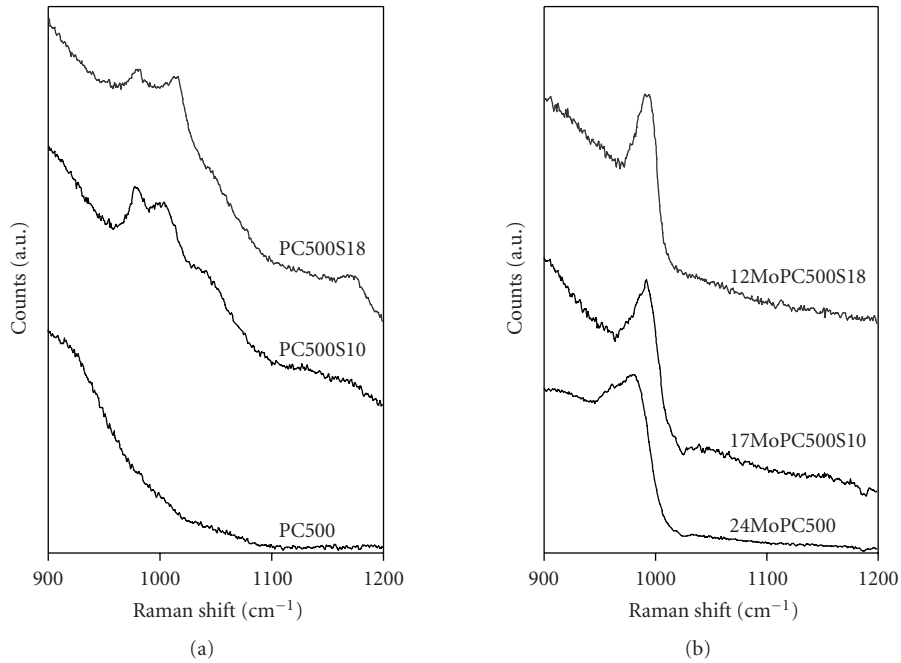

Figure 4: Raman spectra of PC500, PC500S10, PC500S18 (a) and of 24MoPC500, 17MoPC500S10, 12MoPC500S18 (b) catalysts.

The upshift of Mo=O band up to 980 cm^{-1} at increasing sulphate surface density indicates a progressive polymerization of MoO_x species.

3.2. Photocatalytic tests

Preliminary tests carried out in absence of UV light evidenced that no reaction occurred in dark conditions. Cyclohexane conversion and CO_2 outlet concentration on PC500, PC500S10, and PC500S18 as a function of irradiation time are reported in Figure 5. CO_2 was the only product detected in the gas phase (100% selectivity), reaching steady state values after about 30 minutes. Cyclohexane conversion to CO_2 decreases with the sulphate content.

For all titania catalysts, the total oxidation of cyclohexane to CO_2 and H_2O occurs without formation of by-products. Moreover, from Figure 6 it is evident that both cyclohexane consumption and CO_2 formation rates decreased with the sulphate surface density as previously observed in a gas-solid fixed bed photo reactor [15]. This behavior may be explained taking into account the reaction mechanism of gas-solid photocatalytic oxidation of cyclohexane to CO_2 on titania catalyst [31]. In the photocatalytic process, in fact, the surface hydroxyl groups trap the charge transfer to produce very reactive surface hydroxyl radicals. However, the presence of sulphate, grafted to the surface by reaction with hydroxyl groups, decreases their surface concentration, resulting in reduced activity. In addition, it is worthwhile to note that for total oxidation of hydrocarbons on titania the rehydroxylation of the surface is an essential step. Xie et al. [32], studying the gas-solid photocatalytic oxidation of heptane on sulphated and unsulphated titania in the presence of water, found that the presence of SO_4^{2-} was detrimental to the rehydroxylability of the catalyst.

Cyclohexane conversion and benzene outlet concentration as a function of irradiation time on MoPCS catalysts are reported in Figure 7. The analysis of outlet products disclosed the presence of benzene and cyclohexene, the absence of carbon dioxide and the stability of catalyst activity during the photocatalytic test. The trend of cyclohexene concentration (not reported) was similar to that of benzene but its concentration was very low (<1 ppm). It is evident that both cyclohexane total conversion and partial conversion to benzene are strongly dependent of sulphate and molybdate content.

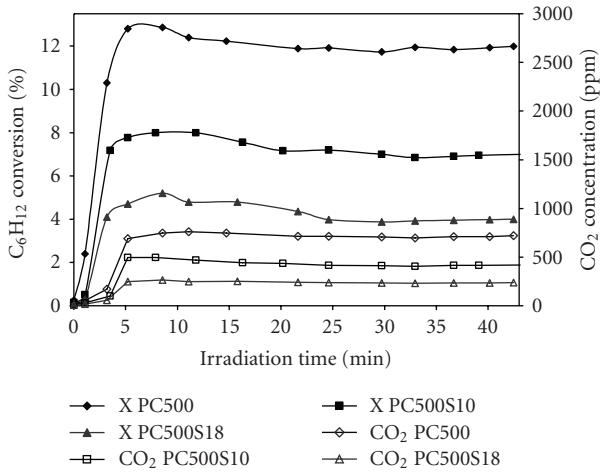

Figure 5: Cyclohexane conversion (X) and CO_2 outlet concentration (CO_2) as a function of irradiation time on PC500, PC500S10, and PC500S18.

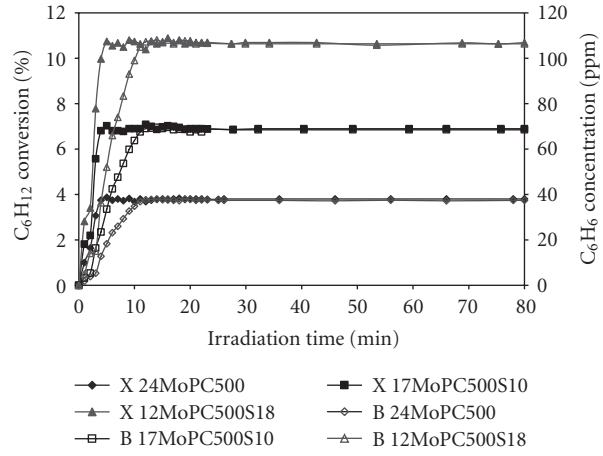

Figure 7: Cyclohexane conversion (X) and benzene outlet concentration (B) on 24MoPC500, 17MoPC500S10, and 12MoPC500S18 as a function of irradiation time.

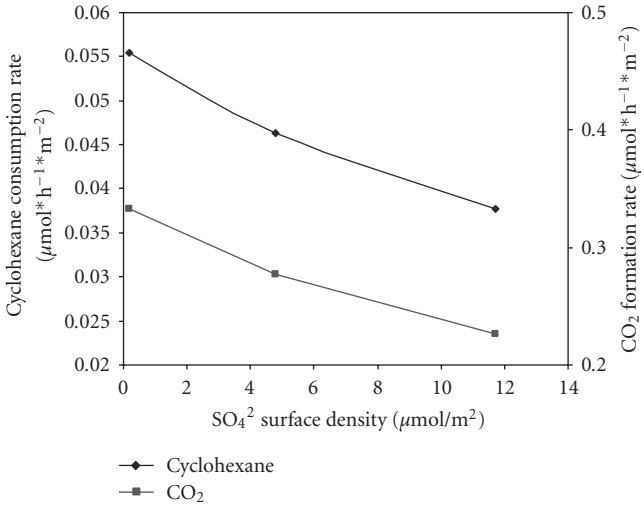

Figure 6: Cyclohexane consumption rate and CO_2 formation rate on PC500, PC500S10, and PC500S18 as a function of sulphate surface density.

The catalytic activity of MoPCs samples is reported in Figure 8(a) in terms of reaction rate per unit surface against sulphate surface density. Since the catalysts have the same molybdate surface density, it is evident that the catalytic activity is only dependent of the sulphate density. The values of cyclohexane consumption rate and benzene formation rate are almost coincident (about 100 % selectivity as the reaction rate to cyclohexene is two orders of magnitude lower) and linearly increase with sulphate density. We previously showed that the very high selectivity to benzene of MoO_x/TiO_2 photocatalyst is related to the coverage extent of titania surface by the polymolybdate species [10].

We retain that the mechanism for the photooxidative dehydrogenation of cyclohexane [19] involves photoexcited octahedral molybdate surface species, which are able to initiate the oxidative dehydrogenation of adsorbed cyclohexane through hydrogen abstraction forming cyclohexene, further dehydrogenated to benzene which finally desorbs from catalyst surface. Photoreduced molybdate is then regenerated by reactive oxygen species, as O^- formed by the reaction between lattice oxygen and positive hole, O_2^- formed from gaseous oxygen and electron of the conduction band, H_2O_2 generated from $OH^\bullet$ coupling. H_2O_2 is also responsible for water formation by decomposition. In summary, the formation of benzene may occur mainly according to a photocatalytic cycle that involves the molybdate both in the oxidized and in the photoreduced forms (redox mechanism) [19]. Cyclohexane may be totally oxidized into CO_2 and H_2O on unselective sites of the titania surface, according to the mechanism presented by Einaga et al. [31]. The presence of sulphate on titania is reported to give higher photoefficiency, in dependence of both energy required to excite the electrons from the valence to the conduction band (Eg) and limiting electron-hole pair recombination owing sulphate electron withdrawing properties. The equivalent band gap energy trend with sulphate content (Table 2) is in contrast with the first point. Further, hypotheses on the role of surface sulphate consider it to participate in the reoxidation step of the surface octahedrally coordinated polymolybdate or to promote hydrogen abstraction from adsorbed cyclohexane molecules, since its acid properties [19].

A strong indication on the main action of sulphate is suggested by Figure 8(b), where the amount of cyclohexane adsorbed in the dark on MoPCs catalysts is reported as a function of sulphate surface density. The linear raise of adsorbed amounts parallels the increase of cyclohexane reaction rate (Figure 8(a)).

The values of ZPC reported in Figure 8(b) also indicate that the adsorption of cyclohexane is correlated to the corresponding increase of catalyst acidity. These results suggest that sulphate doping facilitates hydrogen abstraction from adsorbed cyclohexane, increasing its storage.

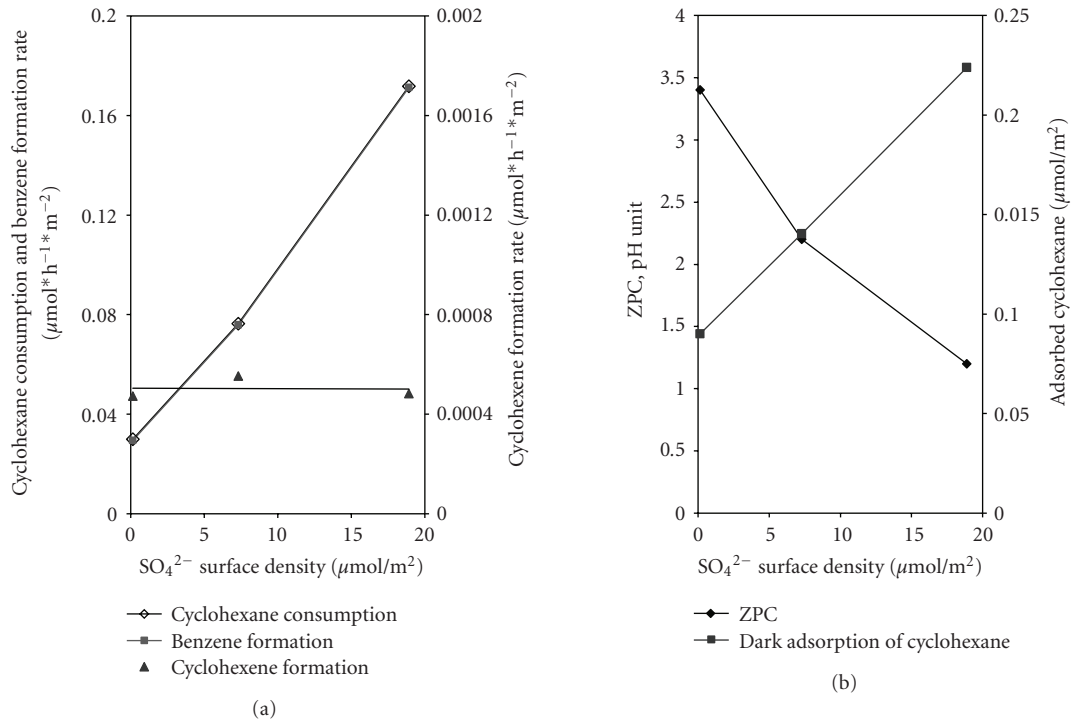

Figure 8: Cyclohexane consumption rate, benzene and cyclohexene formation rate (a) ZPC values and dark adsorption of cyclohexane (b) as function of sulphate surface density on 24MoPC500, 17MoPC500S10, and 12MoPC500S18.

4. CONCLUSIONS

Nanosized titania was employed to explore the effect of sulphate doping on TiO_2 and MoO_x/TiO_2 catalysts for the photooxidative dehydrogenation of cyclohexane in a photocatalytic gas-solid fluidized bed reactor. The high specific surface area of titania, even at 60% of MoO_x surface coverage, allowed to vary sulphate surface density up to 19 μmol/m^2 without formation of segregated MoO_3 crystallites.

On nanosized titania, deep oxidation of cyclohexane only occurred. The cyclohexane consumption rate and carbon dioxide formation rate decreased as the sulphate load increases likely due to the detrimental decrease of surface free hydroxyls.

Photocatalytic selective oxidation of cyclohexane to benzene on MoO_x/nanosized titania was enhanced by the sulphation. The presence of sulphate species on the surface of titania promoted benzene yield as more as higher was the sulphate content. Cyclohexene was produced in low concentration and CO_2 was not detected in gas-phase. The enhanced photooxidative dehydrogenation activity of MoO_x/TiO_2 catalysts is attributed to the increase of surface acidity due to sulphate doping that induces the formation of acid sites able to increase the hydrocarbon adsorption.

ACKNOWLEDGMENT

The authors thank Millenium Inorganic Chemicals for providing nanotitania samples.

REFERENCES

[1] L. Palmisano and A. Sclafani, "Thermodynamics and kinetics for heterogeneous photocatalytic processes," in *Heterogeneous Photocatalysis*, M. Schiavello, Ed., John Wiley & Sons, West Sassex, UK, 1997.

[2] G. Martra, S. Coluccia, L. Marchese, et al., "The role of H_2O in the photocatalytic oxidation of toluene in vapour phase on anatase TiO_2 catalyst a FTIR study," *Catalysis Today*, vol. 53, no. 4, pp. 695–702, 1999.

[3] G. Marcì, M. Addamo, V. Augugliaro, et al., "Photocatalytic oxidation of toluene on irradiated TiO_2: comparison of degradation performance in humidified air, in water and in water containing a zwitterionic surfactant," *Journal of Photochemistry and Photobiology A: Chemistry*, vol. 160, no. 1-2, pp. 105–114, 2003.

[4] V. Augugliaro, S. Coluccia, V. Loddo, et al., "Photocatalytic oxidation of gaseous toluene on anatase TiO_2 catalyst: mechanistic aspects and FT-IR investigation," *Applied Catalysis B: Environmental*, vol. 20, no. 1, pp. 15–27, 1999.

[5] H. Cui, K. Dwight, S. Soled, and A. Wold, "Surface-acidity and photocatalytic activity of Nb_2O_5/TiO_2 photocatalysis," *Solid State Chemistry*, vol. 115, no. 1, pp. 187–191, 1995.

[6] X. Fu, Z. Ding, and W. Su, "Structure of Titania-Based Solid Superacids and Their Properties for Photocatalytic Oxidation," *Chinese Journal of Catalysis*, vol. 20, p. 321, 1999.

[7] D. S. Muggli and L. Ding, "Photocatalytic performance of sulfated TiO_2 and Degussa P-25 TiO_2 during oxidation of organics," *Applied Catalysis B: Environmental*, vol. 32, no. 3, pp. 181–194, 2001.

[8] T. Tanaka, S. Takenaka, T. Funabiki, and S. Yoshida, "Selective photooxidation of propane to propanone over alkali-ion-modified silica-supported vanadium oxides," *Chemistry Letters*, vol. 23, no. 9, p. 1585, 1994.

[9] K. Wada, H. Yamada, Y. Watanabe, and T.-A. Mitsudo, "Selective photo-assisted catalytic oxidation of methane and ethane to oxygenates using supported vanadium oxide catalysts," *Journal of the Chemical Society - Faraday Transactions*, no. 94, pp. 1771–1778, 1998.

[10] P. Ciambelli, D. Sannino, V. Palma, and V. Vaiano, "Photocatalysed selective oxidation of cyclohexane to benzene on MoO_x/TiO_2," *Catalysis Today*, vol. 99, no. 1-2, pp. 143–149, 2005.

[11] F. Amano and T. Tanaka, "Propylene oxide synthesis and selective oxidation over supported metal oxide photocatalysts with molecular oxygen," *Chemistry Letters*, vol. 35, no. 5, pp. 468–473, 2006.

[12] X. Li and C. Kutal, "Photocatalytic selective epoxidation of styrene by molecular oxygen over highly dispersed titanium dioxide species on silica," *Journal of Materials Science Letters*, vol. 21, no. 19, pp. 1525–1527, 2002.

[13] P. Ciambelli, D. Sannino, V. Palma, S. Vaccaro, and V. Vaiano, "Selective oxidation of cyclohexane to benzene on molybdena-titania catalysts in fluidized bed photocatalytic reactor," *Studies in Surface Science and Catalysis*, vol. 172, p. 453, 2007.

[14] P. Ciambelli, D. Sannino, V. Vaiano, V. Palma, and S. Vaccaro, "Catalyzed photooxidative dehydrogenation of cyclohexane to benzene in a fluidized bed reactor," in *Proceedings of the 7th World Congress of Chemical Engineering*, Glasgow, UK, July 2005.

[15] P. Ciambelli, D. Sannino, V. Palma, and V. Vaiano, "Cyclohexane photocatalytic oxidative dehydrogenation to benzene on sulphated titania supported MoO_x," *Studies in Surface Science and Catalysis*, vol. 155, pp. 179–187, 2005.

[16] P. Ciambelli, D. Sannino, V. Palma, et al., "Tuning the selectivity of MoO_x supported catalysts for cyclohexane photo oxidehydrogenation," *Catalysis Today*, vol. 128, no. 3-4, pp. 251–257, 2007.

[17] C. Anderson and A. J. Bard, "Improved photocatalytic activity and characterization of mixed TiO_2/SiO_2 and TiO_2/Al_2O_3 materials," *Journal of Physical Chemistry B*, vol. 101, no. 14, pp. 2611–2616, 1997.

[18] J. S. Noh and J. A. Schwarz, "Estimation of the point of zero charge of simple oxides by mass titration," *Journal of Colloid and Interface Science*, vol. 130, no. 1, pp. 157–164, 1989.

[19] V. Vaiano, *Heterogeneous photocatalytic selective oxidation of cyclohexane*, Ph.D. thesis, 2006.

[20] T. Jin, T. Yamaguchi, and K. Tanabe, "Mechanism of acidity generation on sulfur-promoted metal oxides," *Journal of Physical Chemistry*, vol. 90, no. 20, pp. 4794–4796, 1986.

[21] M. Bensitel, O. Saur, J.-C. Lavalley, and B. A. Morrow, "An infrared study of sulfated zirconia," *Materials Chemistry and Physics*, vol. 19, no. 1-2, pp. 147–156, 1988.

[22] M. Waqif, J. Bachelier, O. Saur, and J.-C. Lavalley, "Acidic properties and stability of sulfate-promoted metal oxides," *Journal of Molecular Catalysis*, vol. 72, no. 1, pp. 127–138, 1992.

[23] H. G. El-Shobaky, M. Mokhtar, and A. S. Ahmed, "Effect of MgO-doping on solid-solid interactions in MoO_3/Al_2O_3 system," *Thermochimica Acta*, vol. 327, no. 1-2, pp. 39–46, 1999.

[24] P. Ciambelli, M. E. Fortuna, D. Sannino, and A. Baldacci, "The influence of sulphate on the catalytic properties of V_2O_5-TiO_2 and WO_3-TiO_2 in the reduction of nitric oxide with ammonia," *Catalysis Today*, vol. 29, no. 1–4, pp. 161–164, 1996.

[25] K. Nakamoto, *Infrared and Raman Spectra of Inorganic and Coordination Compounds*, John Wiley & Sons, New York, NY, USA, 4th edition, 1985.

[26] S. M. Jung and P. Grange, "Characterization and reactivity of pure TiO_2-SO_4 SCR catalyst: influence of SO_4 content," *Catalysis Today*, vol. 59, no. 3, pp. 305–312, 2000.

[27] C. Martin, M. J. Martin, and V. Rives, "Oxidation catalysts obtained by supporting molybdena on silica, alumina and titania," *Studies in Surface Science and Catalysis*, vol. 72, p. 415, 1992.

[28] I. E. Wachs, "Raman and IR studies of surface metal oxide species on oxide supports: supported metal oxide catalysts," *Catalysis Today*, vol. 27, no. 3-4, pp. 437–455, 1996.

[29] M. Cheng, F. Kumata, T. Saito, T. Komatsu, and T. Yashima, "Preparation and characterization of Mo catalysts over AlMCM-41/γ-Al_2O_3 extruded supports," *Applied Catalysis A: General*, vol. 183, no. 1, pp. 199–208, 1999.

[30] J. Twu, C. J. Chuang, K. I. Chang, C. H. Yang, and K. H. Chen, "Raman spectroscopic studies on the sulfation of cerium oxide," *Applied Catalysis B: Environmental*, vol. 12, no. 4, pp. 309–324, 1997.

[31] H. Einaga, S. Futamura, and T. Ibusuki, "Heterogeneous photocatalytic oxidation of benzene, toluene, cyclohexene and cyclohexane in humidified air: comparison of decomposition behavior on photoirradiated TiO_2 catalyst," *Applied Catalysis B: Environmental*, vol. 38, no. 3, pp. 215–225, 2002.

[32] C. Xie, Z. Xu, Q. Yiang, et al., "Comparative studies of heterogeneous photocatalytic oxidation of heptane and toluene on pure titania, titania—silica mixed oxides and sulfated titania," *Journal of Molecular Catalysis A*, vol. 217, no. 1-2, pp. 193–201, 2004.